Power Optimization Configurations in Piezoelectric Energy Harvesting Systems

by

Kristen Thompson

Submitted in Partial Fulfillment of the Requirements

for the Degree of

Master of Science in Engineering

in the

Electrical Engineering

Program

YOUNGSTOWN STATE UNIVERSITY

December 2020

Power Optimization Configurations in Piezoelectric Energy Harvesting Systems

Kristen Thompson

I hereby release this thesis to the public. I understand that this thesis will be made available from the OhioLINK ETD Center and the Maag Library Circulation Desk for public access. I also authorize the University or other individuals to make copies of this thesis as needed for scholarly research.

Signature:

____

Kristen Thompson, Student | Date

Approvals:

____

Frank X Li, Thesis Advisor | Date

____

Mike Ekoniak, Committee Member | Date

____

Eric MacDonald, Committee Member | Date

____

Dr. Salvatore A. Sanders, Dean of Graduate Studies | Date

ABSTRACT

Energy harvesting research from vibration gained great interest for its potential to excel in lower power applications. Often piezoelectric devices are implemented and harness the vibrational frequency as a means to excite the component. The piezoelectric device converts mechanical strain into electrical charge and exists in various prototypes. The cantilevered beam and performance are dependent on the material configuration, size, shape, and layers. This thesis analyzes several piezoelectric components to determine the best way for power optimization and efficiency in this conversion. Store purchased piezoelectric components were soldered and assembled electrically in series or parallel. To increase energy harvesting efficiency at different frequencies, which exist primarily from an ambient source, the output prototype was analyzed.

Table of Contents

List of Figures

Table

List of terms

A – Area of plate
D – Charge Density Displacement
D – Electric Flux Density
d – displacement of parallel plate capacitors
d_{ij} – Charge constant
E – Electric Field
ε – Permittivity
ε_o – Permittivity of free space
f_a – Anti-Resonance Frequency
f_m – Minimum impedance Frequency
f_n – Maximum impedance
f_o – Resonant frequency of cantilever (without load)
f_r – Resonance Frequency (min impedance)
f_s – Resonance Frequency (max impedance)
g_{ij} – Voltage constant
k_{ij} – Coupling Factor
k_T – Stiffness of Piezoelectric
m_{eff} – Mass of the device
Q – Charge
S – Strain
T - Material Stress
V- Voltage

Acknowledgement

I want to extend a sincere thank you to all of those that have helped me in my academic journey at Youngstown State. To my supervisor, Dr. Frank Li, for his guidance throughout my graduate studies. I would like to acknowledge both committee members Dr. Eric MacDonald, and Dr. Mike Ekoniak for their continued support throughout this process.

To my work colleagues at Goodyear, your expertise throughout my internship was invaluable. You all taught me the importance of continuous education and your insightful feedback allowed me to be where I am today.

To my parents, for your continued love and support that you have always given me. Thank you for your unwavering support and continuous encouragement throughout my years of study. I could not have completed this without the support of my friends, Jess, Nadine, and Marina for their distractions to ease my mind outside of research. I appreciate you ladies and am so thankful for our friendship.

Chapter 1 Research Areas

1.1 Project Objectives

The opportunity for the research presented studies the power output performance and energy conversion efficiency of various piezo elements within a mathematical model. To overcome barriers of inefficient power outputs, many researchers explored ways to maximize efficiency and bandwidth by studying the impacts of different piezo materials, design configurations, and other optimization techniques [13][14][29]. If this were to become more effective in producing a consistent output, it can easily be adapted into as a power source for low power electronic devices. The compression or stretching of the piezoelectric component results in the dipole orientation to align themselves along the axis of the crystal, leads to a net polarization across the surface.

Energy harvesting processes derive this energy and harness it to be used for low power applications. The implications of utilizing renewable energy create a less detrimental impact on the environment and are less harmful in their CO_2 emissions. Batteries often need to be replaced, but the duration of time they last depend on the application it is being used for. Advancements in the development of lithium-ion battery technology greatly impacted the automotive industry and production of electric vehicles. There are a wide range of damaging implications as a result of battery production, making energy harvesting an attractive option to reduce energy consumptions [7][11].

Vibration exists in everyday environments and is a viable option to exploit this energy using the piezoelectric effect which converts the mechanical stress to electrical charge.

1.2 Research Question

The main research in question is accurately characterizing the performance of piezoelectric elements. Low power applications are easily sourced through artificial sources such as vibration. Piezoelectric components exist in a variety of configurations, types of materials, and orientations with respect to the 3D plane that all impact the dipole excitations created from the mechanical strain induced. An EMF, electromagnetic field is applied across the crystal material, producing a voltage across it.

Covid-19 resulted in the mathematical model analysis to compare the piezo element behaviors on an equivalent model. The original concept of this research was to validate and analyze road vibrations as well as tire deformation. This deformation on the piezo element was to be characterized and tested to determine if it was able to power a TPMS system. However, the research question of this thesis deviated due to remote learning with the pandemic. Instead, experimental setups are used to demonstrate this concept in a working model. This study examines the vibrational output relative to the spring mass system based on the frequency of excitation [15]. The magnitude of the frequency varies depending on the environmental setting, and there is interest in exploring ways to harvest wasted energy not captured from those vibrations. There are concerns related to if the energy harvester can effectively generate enough charge under excitations.

Project Objectives:

- Predict output of piezoelectric harvester and analyze the influence of design fabrication parameters on performance
- Experimental setup notating power optimization techniques of the piezoelectric component.

Therefore, methodologies that pertain to power optimization performance of the energy harvesting devices are explored. The design, harvesting materials, optimization techniques from the resonance frequencies are reviewed and discussed.

1.3 Thesis overview

As stated above, Chapter 1 establishes the topic area of investigation and the performance of piezoelectric devices. The introductory chapter expresses the purpose of this research study as well as the goals and objectives of this research.

The following chapter further defines energy harvesting concepts and background information. It provides an overview of energy harvesting history and explores three main types, electrostatic, electromagnetic, and piezoelectric. Potential applications prove to be beneficial for the areas of wearable technology and the automotive industry specifically.

The third chapter is the literature review portion of piezoelectricity as it defines the material parameters, configurations, and the component's geometry. These factors greatly influence output performance based on vibrational excitations. It is further discussed the important of matching the vibration oscillations to the resonant frequency to the energy harvesting component to maximize the output. More importantly, is the conversion of this output to prevent energy loss.

The fourth chapter is the experimental setup and measurements obtained. Using an oscilloscope, vibration shaker table, and function generation the performance is characterized. The results are highlighted in this section.

Lastly, the fifth chapter emphasizes the results and relates this back to the research. The experimental outcomes are discussed compared to other analytical studies. There is a list of suggestions for further research and development on this topic.

Chapter 2 Energy Harvesting

2.1 Introduction

Energy harvesting can be defined as the conversion of usable energy from natural resources (ie, power, thermal, wind, ambient energy) into electrical charge that is stored for powering small, wireless devices. Solar energy panels can harvest solar power at a rate of 1000 Watts/m^2 in direct sunlight, however this is dependent on external factors like the weather, season, and even the sunlight angle. With these factors into consideration the typical output power is roughly 40mW per square inch. If the panel is in indirect sunlight the performance reduces significantly [2].

Acoustic sound is another popular option but tends to have drawbacks based on the resonant frequency output from the acoustic wave oscillations. The theory behind this is based on Faraday's law of electromagnetic inflection where the magnetic flux changes between the movement of the magnet and coil. The configuration of the membrane is attached to the piezoelectric material and the movement is a result of the acoustic wave [19].

Thermoelectric utilizes heat energy to convert the temperature differences into electric voltage from materials with high electrical conductivity. The conversion efficiency is significantly lower at a rate of 5 to 15% conversions in an ideal setting [9].

This research analyzes three particular methods to explore for energy harvesting that consists of piezoelectric, electrostatic, and electromagnetic applications. The study outlined specifically focuses on the piezoelectric method and observes its configurations relative to the output performance. The piezoelectric element when under particular amounts of stress or deformation converts the mechanical strain into electrical energy.

The harvesting aspect captures the energy and is an attractive alternative to battery-operated systems [4]. Harvesting and energy storage inherently have many challenges to ensure that enough power is produced for the application. It is classified under two main sources:

Ambient Sources:

These sources naturally exist within the environment without any external influences such as solar, wind, and light.

Artificial Sources:

The other type consists of energy derived as a result from external sources such as human motion or a mechanical system is considered artificial. For example, the oscillations of vibration exist in a variety of mechanical systems, such as a bike, train, or rotor of a wind generator to name a few examples.

2.2 Electrostatic Energy Harvester

An electrostatic energy harvester is dependent on the change in capacitance within the element. The structure of the variable capacitor generates charge as vibration separates the two plates. The distance between the two plates are either air, or some dielectric material. The device implementation is more appropriate to implement for small scale energy harvesters. However, one drawback of this method is in order to generate an electric field, an external voltage source needs to be applied into the system architecture [4].

2.3 Electromagnetic Energy Harvesting

Whenever current flows through a conductor it produces a magnetic field and the change in the magnetic field will result in an electric current. It is important to understand the fundamental principles of electromagnetism with the relation of external vibrations. Faraday's law states the link between the time varying magnetic flux and voltage induced in the circuit are proportional. Therefore, if there is a closed loop within the conductor, a current is induced. The electromagnetic energy transducer harnesses external vibrations and converts this energy flow into electromagnetic induction.

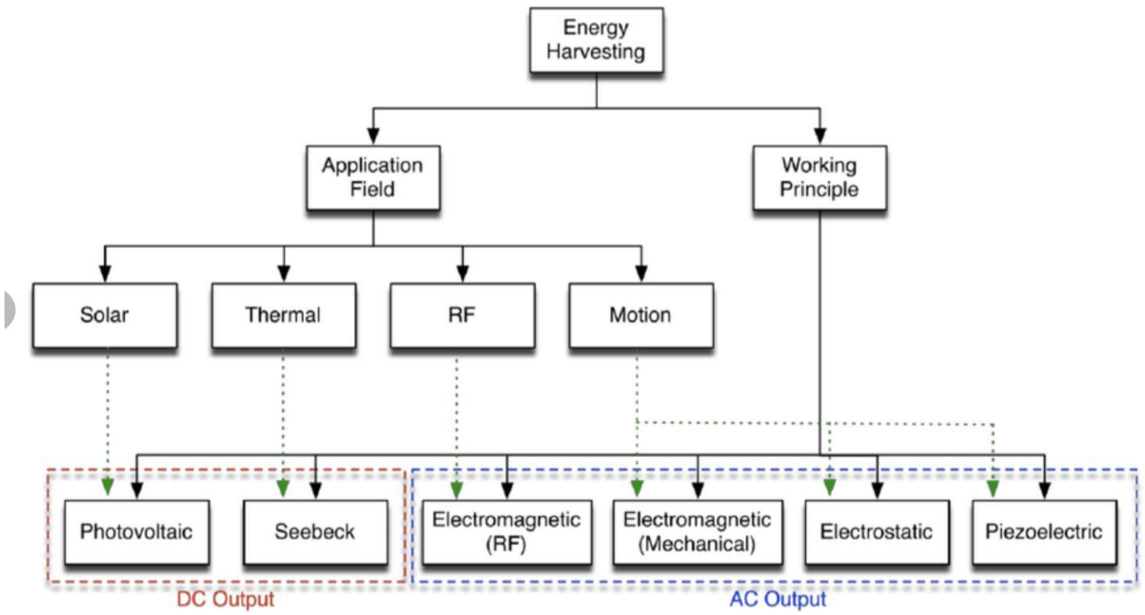

Figure 1: Hierarchy of energy harvesting

2.4 Applications of Energy Harvesting

Energy harvesting is a promising technological advancement that maintains the ability to extend battery life duration as a sustainable alternative. There are many environmental concerns as batteries require periodic replacement or disposal.

Batteries are usually composed of a cathode (positive electrode), anode (negative electrode) and an electrolyte that serves as a conductor placed between the two [3]. As the cell charges and discharges, ions will freely pass between the cathode and anode. For example, during the discharge process, the anode loses electrons as a result of oxidation, but the cathode for simplicity gains those electrons. The electrons create the current flow within a circuit.

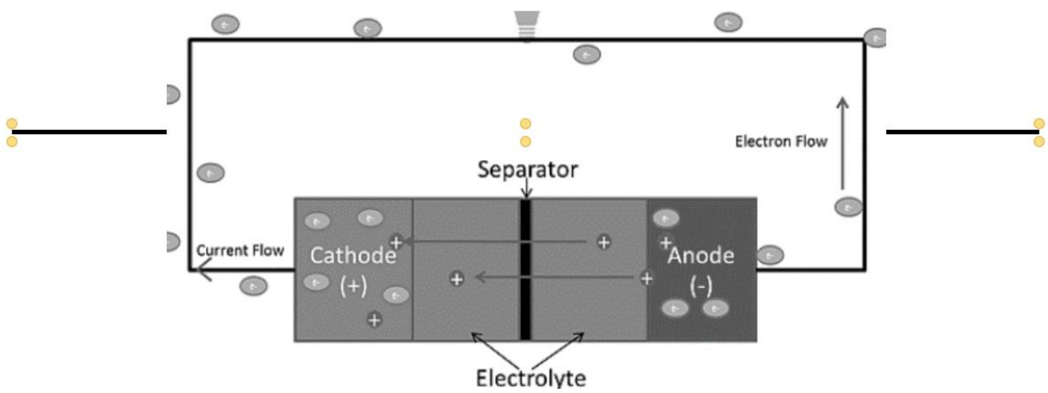

Figure 2: Flow of ions in a rechargeable battery [6]

The concept of a rechargeable battery, or secondary cell, was introduced in 1859 by Gaston Plante, a French physicist. Once this concept was further expanded upon, it became commercially available in 1970 [3]. Most plug-in hybrid electric vehicles (HEVs) and all electric vehicles (EVs) use lithium-ion batteries while the hybrid electric vehicles use Nickel. Recharging a battery can take anywhere from minutes to hours depending on the application, but if charged incorrectly can damage the battery if it reaches max thermal capacity. All batteries have an end to their lifecycle for each charge they lose capacity.

Tire Pressure Monitoring Systems (TPMS)

In the automotive industry, batteries are often used in innovative electric vehicles as well as other important applications such as Tire Pressure Monitoring Systems (TPMS). Car tire monitoring is an important safety feature in any vehicle, and strongly improves the reliability of tire as well as the tire control systems. Development of TPMS is imperative to ensure such safety. More sensors are implemented in remote locations and are often difficult to access.

A typical TPMS system consists of a battery dependent wireless sensor either mounted on the rim, embedded inside, or glued onto the tire, and then contains a remote receiver to collect sensor data. The data collected notifies the driver of low-pressure or potential tire leakage regardless of the TPMS configuration [25].

TPMS valve stems can be mounted several ways with the easiest being on the exterior of the wheel, but it can also be mounted on the inside. If on the interior the tire must be taken off to gain access to the valve stem and sensors. Innovative conceptual designs outline vibrations from the rotating tire and harvesting that energy to extend the battery life of the TPMS sensor or eliminate it completely with placement of piezo components on the inner liner of a tire [30].

Automotive companies can avoid liability issues with a battery-less solution. Batteries normally last 5 years, but in the instance of failure the automotive company can be held liable for repair costs as well as injury since the customer no longer has that safety feature. The flexibility of piezoelectric elements seems suitable for the intelligent tire applications to improve safety/reliability of TPMS systems.

Wearable Technology

Other applications explored consist of wearable electronics with increasing interests in the health and fitness industries to monitor athletic performance. This particular area of research explores the low-power conversion of potential human motion energy to implement into self-powered sensors. Modern day applications in wearable technology suffer developmental challenges [12].

Environmental Impacts

The lithium-ion battery is created from the extraction of toxic, rare earth elements. This particular battery is the primary source in electric vehicle production, but the limitations regarding cost and energy density hinder its competition with an internal combustion engine car. While difficult to compare the two vehicles, electric cars demonstrated a positive environmental impact as they generate less pollutants than that of the average car vehicle by roughly 50% [11]. However, the resources required to source the materials to produce such batteries have a large environmental footprint. Electric car components are composed of lightweight materials such as aluminum or carbon fiber to compensate for the density of the battery. Studies reaffirmed that electric vehicles generate more toxic emissions due to the manufacturing process of obtaining raw materials and contributes twice as much to global warming than that of a combustion engine car [11].

When undergoing the battery at the end of the life cycle it undergoes the decomposition process. This photochemical reaction releases CO2 emissions undermining efforts to mitigate climate change and reduce fossil-fuel dependence [11]. In addition, lithium is known when outside of the given thermal requirements to combust, releasing toxic gas emissions. The recent venture on environmentally friendly sources of energy opened new doors as piezoelectricity is a valid alternative method to conventional means as it recycles wasted energy. Harvesters have the potential to mitigate the issues associated with batteries including the lifespan, size, and environmental pollution from manufacturing that product [25].

Chapter 3 Piezoelectricity

3.1 Piezoelectric Effect

The piezoelectric effect was demonstrated by brothers Jacque Curie in the late 1800s. The correlation between mechanical stress and electric charge were explored by Antoine Becquerel, but this research was inclusive. The Curie brothers successfully experimented between the mechanical and electrical reactions in crystal materials. They verified their suspicions comparing several materials including quartz, topaz, and tourmaline to name a few. Upon completion of this study, the Curie brothers concluded the mechanical strain on the crystal does indeed result in electric potential. Besides that, they were able to demonstrate the importance of the crystalline orientation to create electrical charge from the mechanical strain. Later, other scientists verified the inverse of this to be true from applying an electric charge to a crystalline structure [21].

The crystal lattice is fundamental to the piezoelectric process in which the material experiences a mechanical force and convert this stress into electric charge [22]. There is a polarization induced across the material. The crystal structure generally has charge balances, where negative and positive charges are separated, but cancel each other out so that the overall charge is neutral [28]. Applying physical strain to the material it will disrupt the charge balance as the crystal lattice deforms, creating electrical charge.

The dipole polarization from the field depends on the orientation and applied stress. This will be further discussed in a later section. As a consequence of this discovery, revolutionary opportunities exist to innovate current technological advancement from the phenomenon of piezoelectricity.

3.1.1 Direct vs Indirect Piezoelectric Effect

The direct piezoelectric effect is defined as the mechanical strain imposed resulting in an electric charge. The *indirect piezoelectric effect* is the inverse when an electric field is applied to the same materials, that it becomes mechanically strained [22].

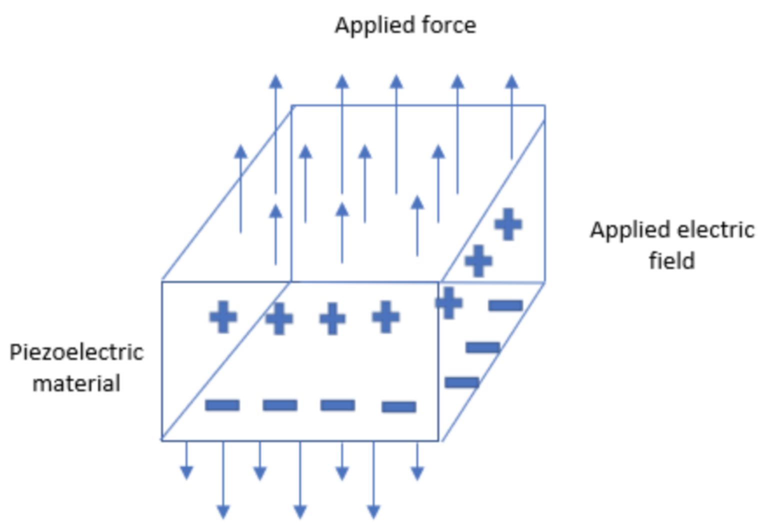

Figure 3: Direct Polarization

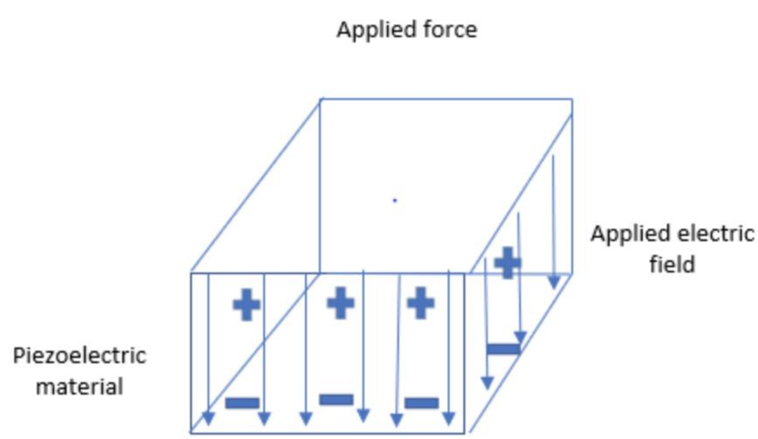

Figure 4: Indirect Polarization

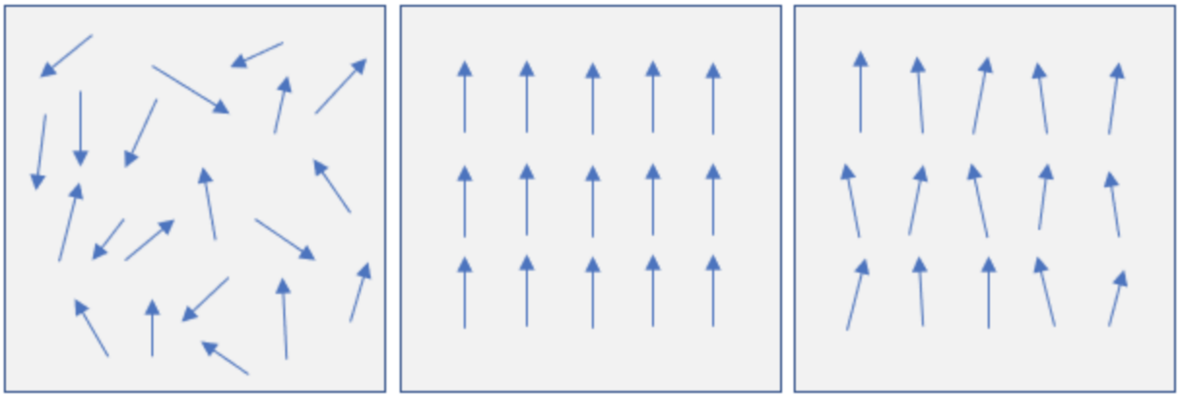

Figure 5: (a) Before poling (b) In poling (c) After polarization

3.2 Piezoelectric Constitutive Equations

The piezoelectric constitutive equations below relate the material of the piezoelectric to the material's stress (T), strain (S), charge-density displacement (D), and electric field (E) interact [21][29][25].

The Linear behavior of the piezoelectric behavior can be defined as:

$$D = \varepsilon E \quad \Longrightarrow \quad D_i = \varepsilon_{ij} E_J \qquad (3.2.1)$$

Where the electric flux density is defined as D. Maxwell equations define that relationship with the electric field as $\nabla \cdot D = 0, \nabla x\ E = 0.$ (3.2.2)

Hooke's law relates the Strain and Stress (T) relationships for linear materials:

$$S = sT \quad \Longrightarrow \quad S_{ij} = s_{ijkl} T_{Jkl} \quad (3.3.3)$$

This is given in equation 2.1

$$\begin{pmatrix} S \\ D \end{pmatrix} = \begin{pmatrix} s^E & d \\ d_t & \varepsilon^T \end{pmatrix} \begin{pmatrix} T \\ E \end{pmatrix} \qquad (3.2.4)$$

Equation 2.1 can be further simplified to derive the indirect and direct piezoelectric effects:

$$S = s^E T + dtE \quad \Rightarrow \quad S_{ij} = s_{ijkl} T_{Jkl} + d_{kij} E_K \ (3.2.5)$$

$$D = dT + \varepsilon^T E. \quad \Rightarrow \quad D_i = d_{ijk} T_{Jk} + \varepsilon_{ij} E_j \quad (3.2.6)$$

Where Epsilon is the permittivity (free body dielectric constant)

$$\varepsilon = \varepsilon_r \varepsilon_o \qquad (3.2.7)$$

ε0 is the permittivity of free space and expressed as:

$$\varepsilon_o = 8.854 \; x \; 10^{-12} Farad/meter$$

Piezoelectric coefficients can be defined as outlined below. The first set correlates with the direct effect while the second set of terms correspond to the indirect effect. The relationships from the two equations above contribute to the following relationships among the parameters below. Where d is the charge developed divided by the stress applied, g is the electric field divided by the applied stress, h is the strain divided by the electric field, and e is the stress developed divided by the electric field.

$$d_{ij} = \left(\frac{dD_i}{dT_j}\right)^E = \left(\frac{dS_j}{dE_i}\right)^T (3.2.8)$$

$$e_{ij} = \left(\frac{dD_i}{dS_j}\right)^E = -\left(\frac{dT_j}{dE_i}\right)^S (3.2.9)$$

$$g_{ij} = -\left(\frac{dE_i}{dT_j}\right)^D \qquad = \left(\frac{dS_j}{dD_i}\right)^T \text{(3.2.10)}$$

$$h_{ij} = -\left(\frac{dE_i}{dS_j}\right)^D \qquad = -\left(\frac{dT_j}{dD_i}\right)^S \text{(3.2.11)}$$

These equations are combined into four coupled equations relating the voltage, charge, stress, and strain relationships.

Strain- Charge Form:

$$S = s^E T + dtE \quad \text{(3.2.12)}$$

$$D = dT + \varepsilon^T E \quad \text{(3.2.13)}$$

Strain-Voltage Form:

$$S = s^D T + gtD \text{ (3.2.14)}$$

$$E = -gT + \varepsilon^{T(-1)} D \text{ (3.2.15)}$$

Stress-Charge Form:

$$T = c^E S - e^t E \text{ (3.2.16)}$$

$$D = eS + \varepsilon^S E \text{ (3.2.17)}$$

Stress-Voltage Form:

$$T = c^D S - q^t E \text{ (3.2.18)}$$

$$E = -qS + \varepsilon^{S(-1)} D \text{ (3.2.19)}$$

3.2.1 Vibration

The ultimate goal to maximize output efficiency is to match the operational frequencies of the harvester with the resonant frequency of the piezoelectric elements. The occurrence of vibrations is experienced in everyday life. The piezoelectric components when exposed to an AC electric field, the piezoelectric output results in oscillations. The resonance frequency is the frequency that most efficiently converts the mechanical energy into electrical energy and vibrates most readily. The minimum impedance frequency f_m occurs at the resonance frequency f_s . The minimum impedance frequency is equivalent to the resonance frequency, f_r.The frequency at maximum impedance, f_n is also known as the anti-resonance frequency f_a [26].

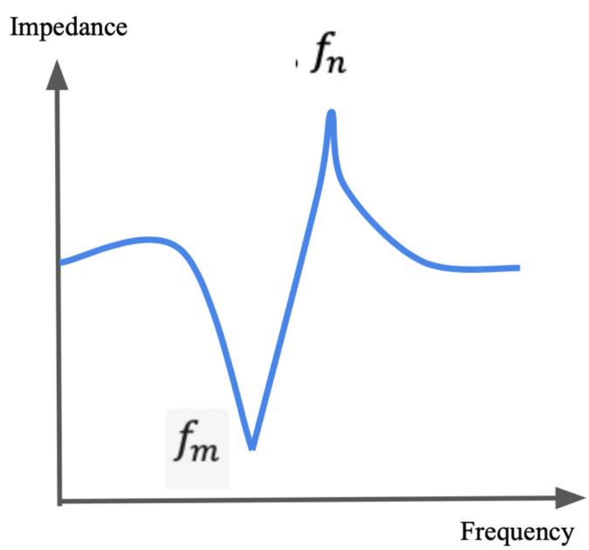

Figure 6: Frequency response with respect to changing impedance

These frequency values can be used to calculate the electromechanical coupling factor, k, later discussed in Chapter 3. It was discovered that many piezoelectric devices in practical applications are used below the resonant frequencies to reduce the phase shift between the signal and actuator. To calculate the resonant frequency of a traditional cantilever piezoelectric energy harvester with a small damping effect use the following equation:

$$f_o = \frac{1}{2\pi}\sqrt{\frac{k_T}{m_{eff}}} \quad (3.1)$$

Where the resonant frequency is defined as f_o without load in Hertz. The stiffness of the piezoelectric is k_T and the mass of the device is m_{eff} [19]. The resonance frequency depends on several factors that will be discussed in later chapters. In the instance there is a load attached to the piezoelectric, it will result in a reduction in the frequency. If the device does not have an attached load, the equation is altered.

Piezo elements can also be regarded as a parallel plate capacitor when operated below the resonant frequencies. Parallel plate capacitors are defined to be a layering of dielectric materials between two plates separated by a distance d [Worthington]. Q is charge, area of the plate is A, D is the charge density, d is the distance between plates and E is the permittivity.

$$D = \frac{Q}{A} \quad (3.2) \qquad\qquad D = -\frac{Q}{A} \quad (3.3)$$

The total electric field between the two plates is derived as:

$$E = \frac{D}{2\varepsilon_0} - \frac{D}{2\varepsilon_0} = 0 \quad (3.4) \qquad\qquad E = \frac{D}{\varepsilon_0} = \frac{Q}{A\varepsilon_0} \quad (3.5)$$

The potential difference between plates is:

$$V = Ed \ (3.6)$$

Substituting Equation 10 into 9 the voltage is now characterized as:

$$V = \frac{Qd}{A\varepsilon_0} \ (3.7)$$

The amount of charge a capacitor can store is given by the equation:

$$Q = CxV \ (3.8)$$

The capacitance of the parallel plate capacitor:

$$C = \frac{Q}{V} = \frac{A\varepsilon_0}{d} \ (3.9)$$

From Equation 3.9, the relationship between the applied force is shown to be directly proportional to the voltage. The voltage is maintained in the poling direction. Whenever the stress is mitigated, the material will expand, and the charge is now in the opposite direction. Equations 3.6 to 3.9 provide calculations for the accumulated charge, voltage produced, and total energy from the applied stress.

3.3 Fundamental Modes of Operation

3.3.1 Charge Constant

As previously mentioned, the stress applied results in movement of the dipoles and direction known as polarization. The two main modes of operation are categorized based on the orientation of the dipoles under two main modes of operation d31 and d33. The electric field (dipole polarization 3) is perpendicular to the applied stress (1) in the d31 mode. In stark contrast, the opposite is true of the d33 mode in which both the applied stress and electric field are within the same direction. The directions of X, Y, and

Z are represented with the subscripts 1, 2, or 3. Please see the figure below to illustrate this orientation [30].

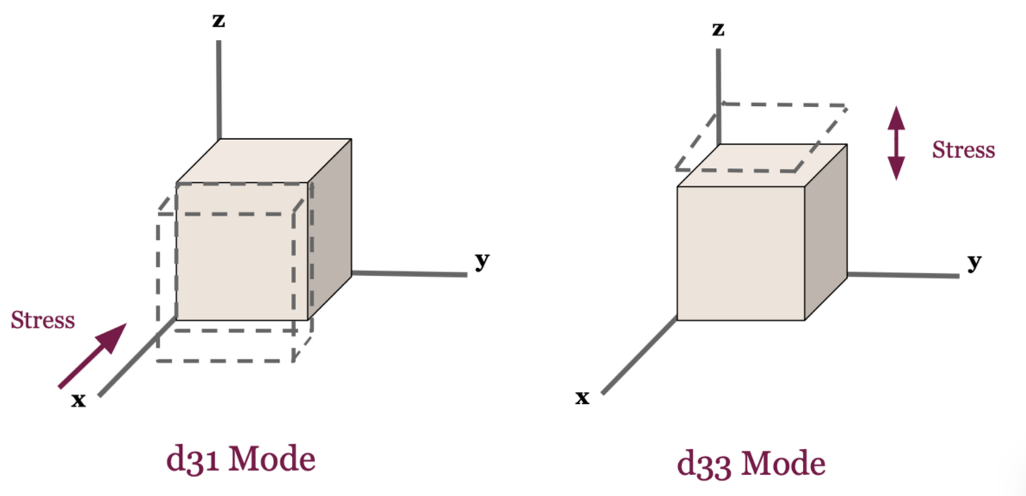

Figure 7: Modes of Operation

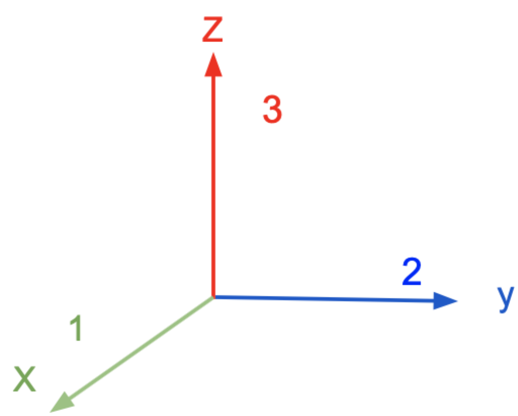

Figure 8: Axis Direction

Equations:

$$d = k\sqrt{S^{E}\varepsilon^{T}} \qquad (3.3.1)$$

$$d_{31} = k_{31}\sqrt{S^{E}{}_{11}\varepsilon^{T}{}_{33}} \qquad (3.3.2)$$

$$d_{33} = k_{33}\sqrt{S^{E}{}_{33}\varepsilon^{T}{}_{33}} \qquad (3.3.3)$$

The piezoelectric constitutive equations outlined the variable parameters without the meaning behind the directions. Elastic compliance, s is the strain received from the amount of forced applied. S^{E} the stress in the direction. For the above, $S^{E}{}_{11}$ is the perpendicular directions from the polarized ceramic component for the stress and strain. $S^{E}{}_{33}$ indicates the strain is polarized were both the stress and electric field are along direction 3. $\varepsilon^{T}{}_{33}$ is the permittivity value of the dielectric in direction 3 [18].

3.3.2 Voltage Constant

The subscript (g) is the piezoelectric voltage constant is achieved from the applied mechanical stress experienced by the piezoelectric component per unit of electrical charge displacement. The directions are maintained similarly as in the charge constant where directions X,Y, and Z are notated with subscripts 1, 2, and 3. The voltage constant is described as the piezoelectric charge constant (d33 or d31) divided by the dielectric constant of the material [18].

Equations:

$$g = \frac{d}{\varepsilon^{T}} \qquad (3.3.4)$$

$$g_{31} = \frac{d_{31}}{\varepsilon^{T}{}_{33}} \qquad (3.3.5)$$

$$g_{33} = \frac{d_{33}}{\varepsilon^{T}{}_{33}} \qquad (3.3.6)$$

3.3.3 Electromechanical Coupling Factor k

The coupling factor, k_{ij} is defined as the measurement and effectiveness from the conversion of mechanical strain into electrical charge. This particular subscript refers to a one-dimensional geometry on the element, while k_{eff} is for any orientation. The following equations explain the calculation to obtain this value for different material parameters.

Coupling Factor Mode (k)	Frequencies	Formula	Equation #
${k_{31}}^2$	Static/Low	$= \frac{{d_{31}}^2}{{S^E}_{11}{\varepsilon^T}_{33}}$	(3.3.7)
${k_p}^2$	Static/Low	$= \frac{2{d_{31}}^2}{({S^E}_{11}+{S^E}_{12}){\varepsilon^T}_{33}}$	(3.3.8)
${k_{33}}^2$	Static/Low	$= \frac{{d_{33}}^2}{{S^E}_{33}{\varepsilon^T}_{33}}$	(3.3.9)
${k_{31}}^2$	High	$= \frac{\left(\frac{\pi}{2}\right)\left(\frac{f_n}{f_m}\right)\tan\left[\left(\frac{\pi}{2}\right)\frac{f_n-f_m}{f_n}\right]}{1+\left(\frac{\pi}{2}\right)\left(\frac{f_n}{f_m}\right)\tan\left[\left(\frac{\pi}{2}\right)\frac{f_n-f_m}{f_n}\right]}$	(3.3.10)
k_p	High	$= \sqrt{\left[\left(2.51\ \frac{f_n-f_m}{f_n}\right)-\left(\frac{f_n-f_m}{f_n}\right)^2\right]}$	(3.3.11)
${k_{33}}^2$	High	$= \left(\frac{\pi}{2}\right)\left(\frac{f_n}{f_m}\right)\tan\left[\left(\frac{\pi}{2}\right)\frac{f_n-f_m}{f_n}\right]$	(3.3.12)

$k_{eff}{}^2$	Any shape	$= (\frac{f_n{}^2 - f_m{}^2}{f_n{}^2})$	(3.3.13)

Table 1: Coupling Factor Equations

The coupling factor k_{33} is parallel to the polarized piezoelectric element in direction 3 and the vibrations oscillate in the same direction. The other subscript k_{31} denotes the vibrations are perpendicular to the polarized component and travel in direction 1. These values for k are calculated from the frequencies f_m (minimum impedance) and f_n (maximum impedance). The relationship between those variables are demonstrated in Table x for higher frequencies [18][23].

3.4 Configuration of Piezoelectric Energy Harvesters

Bimorph or unimorph cantilever

The configuration of the piezoelectric components and materials impacts the design performance. The resonant frequency is when the natural vibration frequency of the system matches that of the applied frequency of oscillation as described earlier. The frequency varies depending on the material, size, and structure type of the piezo. It is often difficult to match the resonance frequency with that of the system due to varying conditions and complex parameters that must be taken into consideration. The cantilever beam consists of different piezoelectric layers or materials as well as an elastic layer usually. There are structurally many diverse layer types [30][29].

The cantilever beam piezoelectric primarily has three different configurations, unimorph, bimorph and parallel series.

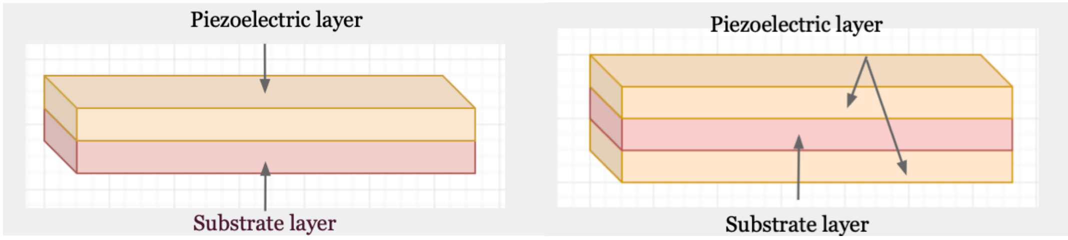

Figure 9: Piezoelectric Configurations a.) Unimorph b.) Bimorph

The unimorph is easily fabricated using the lead zirconate titanate (PZT) and polyvinylidene fluoride (PVDF). It only has one piezoelectric layer on the substrate. Since there is only one piezoelectric layer the output is significantly lower than that of a bimorph.

The bimorph cantilever-type vibration energy harvester contains an elastic layer that is placed in between two piezoelectric layers. The bimorph configuration maintains a neutral axis in the center of the device without regard to the component's material or dimensions. Research indicated the increase in the film thickness resulted in increasing the distance between this neutral axis and piezoelectric film layer. Therefore, the amount of deflection experienced from the strain received will generate a power increase. This finding indicates the performance of a bimorph type is significantly more efficient compared to the unimorph type [27].The structure is meant in the bimorph to obtain tension in the top layer while the bottom is compressed in order for there to be more flexibility in the bending mode provided the bimorph is operating as a 31- mode cantilever. This can have multiple layers and the direction of the dipoles is defined as parallel or series polling. The poled piezo, meaning the orientation to their polarity with respect to the charge constant. Therefore, in different axis configurations, the mechanical stress forces are different [1].

The last type is that of the multiple layer configurations of the piezoelectric which consist of multiple different structure styles that do not fit in either the unimorph or bimorph category.

The key factor in energy harvesting from vibration to ensure the vibration frequency matches that of resonant frequency for maximum power transfer. It is proven when the two are mismatched that the power efficiency decreases [20] Often the geometry of the film configuration correlates to the strain distribution across the element. The cantilever rectangular beams are well explored. The bending of the cantilever occurs one end of the device and not the other. Therefore, non-bent end does not contribute to power generation. A cantilever beam like many other geometries experience different modes of vibration, but the lowest resonant frequency is experienced in the first mode of vibration. This provides a higher electrical output as it has more deflection.

Experimental studies are in favor of a triangular shaped cantilever as it distributes a strain that is considered proportional across the cantilever. The linear distribution of strain over the length of the triangular cantilever proves to be a more reliable option [30].

The triangular geometry improved a power output gain of 30% over the rectangular counterparts [20]. It was found the beam shape has little impact on efficiency, but it needs to be factored into the excitation strength received. The material thickness proposed by Paquin indicated a slope angle of a tapered beam increases the power output four times more than if sloped at a lower angle.

3.5 Configuration of the element & materials

3.5.1 Single Crystals

The piezoelectric materials can be classified as single crystal, piezoceramics, thin film piezoelectric, composites, and polymers. The spontaneously polarized, naturally occurring materials like quartz, lithium niobate, lithium tantalite, and tourmaline are single crystals [24][30]. Multiple configurations exist for crystal and the direction in which the dipole is polarized. The single crystals usually vary in magnitude based on the material form and are most commonly used in acoustic sound applications.

3.5.2 Polymers

One of the most popular polymers is the Polyvinylidene difluoride (PVDF) as a result of its large observed output from the placement under a strong electric field. The poling direction mode d33 is a negative value indicating the material will not expand, but rather compress [30].

3.5.3 Ceramic Materials

The most popular material used in single piezoelectric is the PMT-PT type (lead magnesium niobate and lead titanate) and PZT (lead zirconate titanate). The structural analysis of the design is a simple cubic symmetry within the lattice crystal [25][30]. These two material types consist mostly of ceramics and single crystals are a part of the subgroup of piezoelectric components known as “ferroelectrics.”

Tian found in that piezoelectric single crystals and ceramics have a higher mechanical to electrical conversion compared to piezoelectric polymers. The constitutive equations referenced indicate the direction of polarization, coupling factor k, and E permittivity. Piezoceramics are manufactured after heating the powder to a high temperature. PZT, a type of ceramic, has the properties to withstand high critical temperature also known as the Curie temperature. This particular material was modified in chemical composition by altering it to PZT-5H, PZT5-A, PZT-4, and PZT-8 [30].

The table below outlines the significant value difference between crystals/ceramics and polymers confirming the conclusion these composites have better properties [17][30]. One reason for this is because they can withstand a greater mechanical strain as a result of the flexibility. This makes that particular material type well suited for applications that require more bending of the piezoelectric device. The ceramic materials in the table outline the brittle nature and may not be suitable for harsher environments that require more flexibility. For example, tires often experience significant vibrations, mechanical stress, and deformation. A thinner more flexible piezoelectric is required to withstand the environment.

	PZT-4	BaTiO	PZT-5A	PVDF	PMN-PT	PZT-8	PMN-33%PT
d31	-85	-78	-171	-23	-920	-97	-1,400
d33	225	149	374	33	2200	225	2,400
g31 (10^3 Vm/N)	-7.5	5	-11.4	216	-17.1	-11	24.3
g33	8.5	14.1	24.8	330	44	25.4	41.7
k33	.7	0.48	.71	0.15	.93	.64	.93
Curie Temp (degrees C)	328	115	365	100	145	300	145

Table 2: Report of Piezoelectric Materials & Applications [30]

This table outlines the properties of several piezoelectric materials and characterizes their properties. Piezoelectric components of varying material configurations experienced thermal testing in extreme environments with temperature ranges from -150C to 250C [10].

3.6 Piezoelectric Energy Conversion Efficiency

Figure 10: Block diagram of an energy harvesting application

Studies indicate the importance of overcoming conversion limitations. For low power applications the electrical conversion of AC to DC is needed prior to using this harvested energy and ensuring optimal efficiency during the conversion. Piezoelectric elements produce AC voltage and most applications, like an LED needs a DC current. This conversion can be done implementing a bridge rectifier circuit. To verify the conversion is properly taking place, an oscilloscope will be used to visually see the change between AC and DC. It is possible a single rectifier could be used for that conversion. The diode can respond differently to applied voltages of opposite polarities.

Ottman studied the use of a DC to DC converter to optimize the vibrating piezoelectric device. It was concluded the energy harvested amounted to a total of 30.66

mW [17]. The use of the DC to DC converter will amplify the output current and reduce the voltage. Liu conducted a similar experimental study of a 70% efficiency conversion using a quasilinear impedance adaptation technique. The power delivered a 12.3 mW output and harvested power of 3.2 mW [15].

The next step is to use a large capacitor to filter out most of the unwanted noise in the signal. Since the diode does not allow current to flow back through to the transformer, the capacitor discharges through the load resistor with a time constant. Several studies explored adaptive control measures to characterize power lose and provide solutions to improve the conversion from impedance matching.

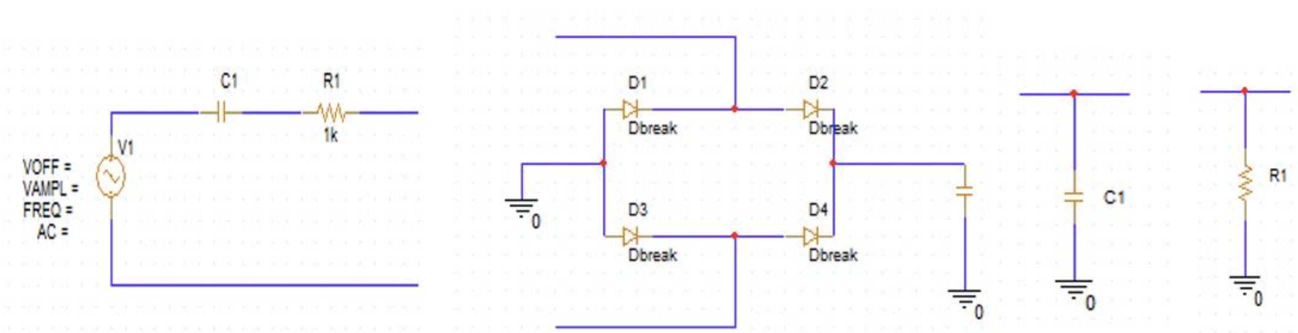

a.) Piezoelectric Component b.) Bridge Rectifier c.) Capacitor d.) Load

Figure 11: Electrical Schematic of the Energy Harvesting Diagram

The principle of impedance matching is characterized as taking the input electrical load or the source and matching the value to the load to obtain the condition of maximum power transfer. Ottman explored the above circuitry diagram utilizing a DC-DC converter to match vibration-based piezoelectric devices. The research states the difference of this device as the internal impedance is capacitive in stark contrast to other variations being inductive. This study concluded the output voltage was at a maximum value whenever the bridge rectifier circuit is slightly less than one-half of the open-circuit voltage of the generator. The point of optimal power was tracked at several points of frequency excitation and varying the resistive load. The study concluded with an open circuit voltage of 45.8V, the max current found was at 4.3mA[17]. The range of the current above 4mA was whenever the duty cycle remained between 2.5-4.5% [OTTMAN]. One experiment consisted using an adaptive controller to adjust the resonance frequency with respect to the load to reduce power conversion loss.

Liu conducted a similar experimental study of a 70% efficiency conversion using a quasilinear impedance adaptation technique [15].

Chapter 4 Methodology

4.1 Initial Investigations

Energy harvesting research aims at increasing the efficiency from wasted sources. Mechanical energy conversions from vibrations are easily fabricated from human motion, vehicles, roadways, pumps, and other structures. Modification of the resonance behavior in previous research indicated better output power performance and improved bandwidth of vibration energy harvesters. The energy density equation will generate a larger power output if the values for the strain constant d, and voltage constant g, will be higher.

4.1.1 Lab EquipmentF

1.) Oscilloscope is a type of electronic test instrument with a graphical user interface to display voltage signals as a function of time. Often used to analyze the output from the waveform include the frequency, period, amplitude, and signal distortion.

2.) Vibration Generator U8556001 – set the frequency of the signal.

3.) Function Waveform Generation (Keysight 33600A)

4.) LCR Meter (Keysight U1733C)

5.) Locked-In Amplifier

6.) Resistor Decade Box

4.1.2 Piezoelectric Elements

Figure 12: Piezoelectric Components SEN 10293

The piezoelectric elements above are the SEN-10293 piezo film from Sparkfun and the plate material is brass. The documentation specifies the dimensions of the plate size to be 12 mm, with a thickness of .22 mm .and maintains a resonance frequency at 9kHz [23]. The unimorph configuration indicates the single layer of substrate across the device, but the two vary in size. The documentation for this widely produced and popular item is listed to generate Another type of piezoelectric was reviewed in the bimorph configuration, but with a rectangular geometry manufactured by Mouser Electronics. The thickness is of the component is 0.46mm. The dimensions for the device are at a length of 55.4 mm, a width of 23.4 mm and the resonance frequency is at 130 Hz [8].

Figure 13: Piezoelectric device S118-J1SS-1808YB

The manufacturing specification sheets indicate the performance output voltage to reach 17.3 V and power at 4.4 mW [8]. This piezoelectric model encapsulates piezo ceramics between copper materials for a robust and electrically insulated solution.

These piezoelectric cantilevers were individually examined with an LCR meter when pressed. The table below demonstrates the performance of each device individually.

Piezo Component	Parts	Voltage Measured (individual)	Current Measured (individual)
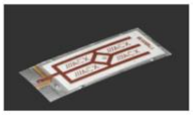	Part # S118-J1SS-1808YB Piezoelectric Bender	9.6V	6.38 mA
	SEN- 10293 Smaller Piezo	2.4V	1.6 mA
	Larger Piezo	8V	.00532 A

Table 3: Piezoelectric Voltage Output

The LCR meter is another important piece of electrical test equipment used to measure the inductance, capacitance, resistance, and impedance of the piezo component at varying frequencies. Measurements were taken to classify the device under test and understand the characters of the component as a function of frequency. The voltage drop across the piezo component divided by the current is the electrical impedance. As previously stated, this is important to distinguish the resonances of the vibration to excite the electrical charge response output from the component. The EMF voltage is proportional across the crystal material. The resonance frequency is the frequency at which the material vibrates and most efficiently converts the mechanical strain to electrical charge.

Large Piezo Parallel	Frequency (Hertz)	L (Hertz)	C (nF)	R (Ohm)	Z (kOhm)
	100	-36.5	69.31	1000.1	23
	120	-25.28	68.69	840.8	19.286
	1000	-.000386	65.43	134.48	3.429
	10000	-0.000004578	55.22	19.26	0.288
	100000	5.83E-06	-432.2	15.06	0.01534
Small Piezo Parallel	Frequency (Hertz)	L (Hertz)	C (nF)	R (Ohm)	Z (kOhm)
	100	-72.66	34.66	840	2.77
	120	-50.31	34.59	710	2.61
	1000	-0.0007447	33.92	102.57	2.822
	10000	-0.000009992	24.98	20.66	2.838 kOhm
	100000	-0.0000789	32.2	1.686	2.87 kOhm
Large Piezo Series	Frequency (Hertz)	L (Hertz)	C (nF)	R (Ohm)	Z (kOhm)
	100	-497.1	5.107	`.01538	312.1
	120	-344.2	5.039	0.01276	260.4
	1000	-5.263	4.79	1523	33.08
	10000	-0.00006074	4.157	189	3.807
	100000	0.0000825	5.968	109	121.588
Small Piezo Series	Frequency (Hertz)	L (Hertz)	C (nF)	R (Ohm)	Z (kOhm)
	100	-1147.3	2.194	14.062 kOhm	727.5
	120	-794.2	2.1887	11.572 kOhm	605.3
	1000	-11.742	2.146	1785.6 Ohm	74.25
	10000	-0.00015464	1.652	387.2 Ohm	9.71
	100000	-0.0012593	2.015	9.632 Ohm	0.7906

Table 4: LCR Measurements for the inductance, capacitance, resistance, and impedance

Table 4 displays the measured output results from the LCR meter at varying frequencies without any applied strain.

4.1.3 LED Verification:

The produced voltage is proportional to the amount of pressure applied to the piezoelectric element. There is a threshold value where the LED will change its state from low to high. The piezoelectric component performance as a power generator can be determined by taking measurements of the charging and discharging cycle in the output capacitor in the energy harvesting schematic.

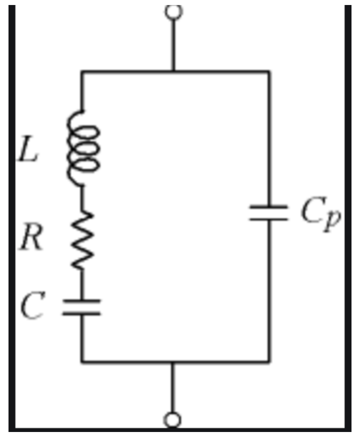

Figure 14: Equivalent circuit of a piezoelectric element

The unimorph piezoelectric elements have considerable limitations in the output power produced and when connected directly to the LED, it would not flash. For the bimorph industrial size piezoelectric bender this was feasible as the direct energy supply to the LED. Therefore, in instances where not enough power is produced, it must be harvested and stored before delivering enough to the LED to change the state of the device.

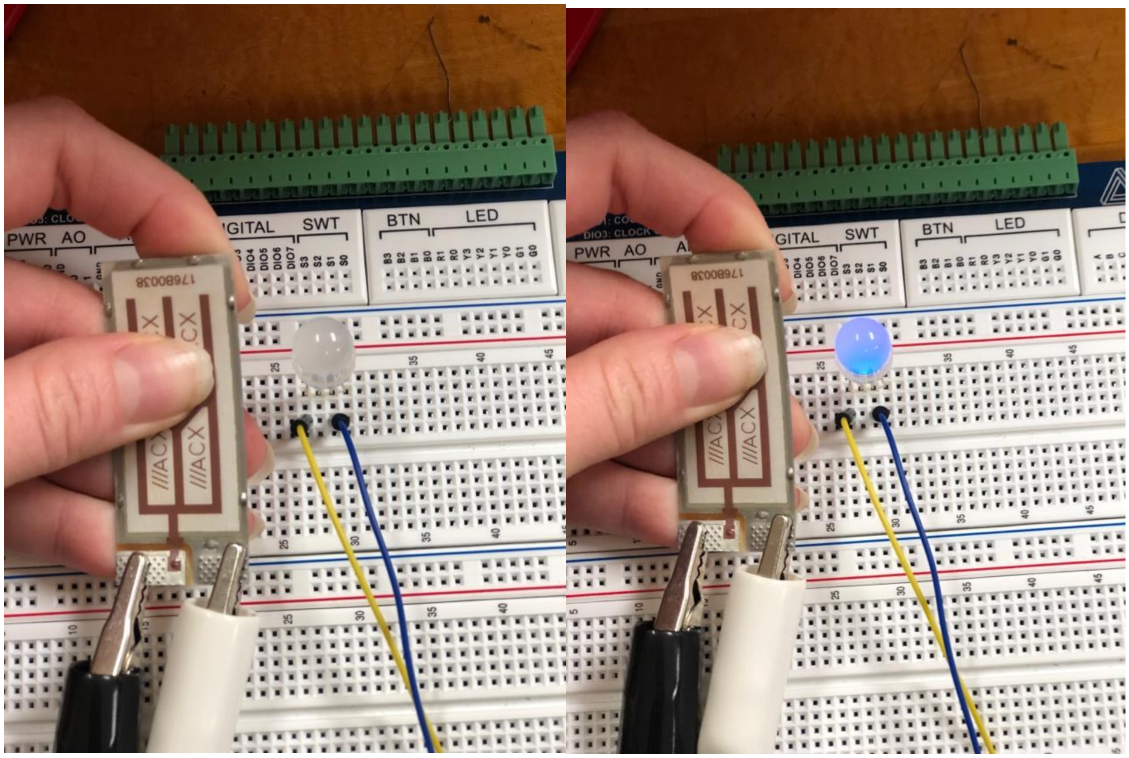

Figure 15: LED Test

The power required by the LED in normal operating conditions requires at least 20 mW of power [29]. In order to increase the power transferred to the LED, more than one piezoelectric bender could be used to raise the harvested power. This can be connected in various combinations like being wired in series, parallel, or a mixture of both series and parallel. This thesis is expanding on the previous works described in [14][15][29][30] and investigates the parallel and series configurations of multiple piezoelectric benders.

Other research based on piezoelectric energying harvesting from vibration using the piezoelectric device as a power generator. There is considerable evidence with connecting multiple piezoelectric cantilevers to improve power performance output when connected in alternating polarities.

4.2 Experimental Setup

The experimental setup is as follows for the piezoelectric device (SEN-10923) from spark fun [23]. The dimensions of the cantilever are shown in the figure. A vibration shaker was used in connection with the oscilloscope to measure the output of the device. A lock in amplifier was added to reduce signal noise by extracting the carrier wave signal from the environment. The vibration table is representative of ambient sources in the environment and is set over a wide range of frequencies.

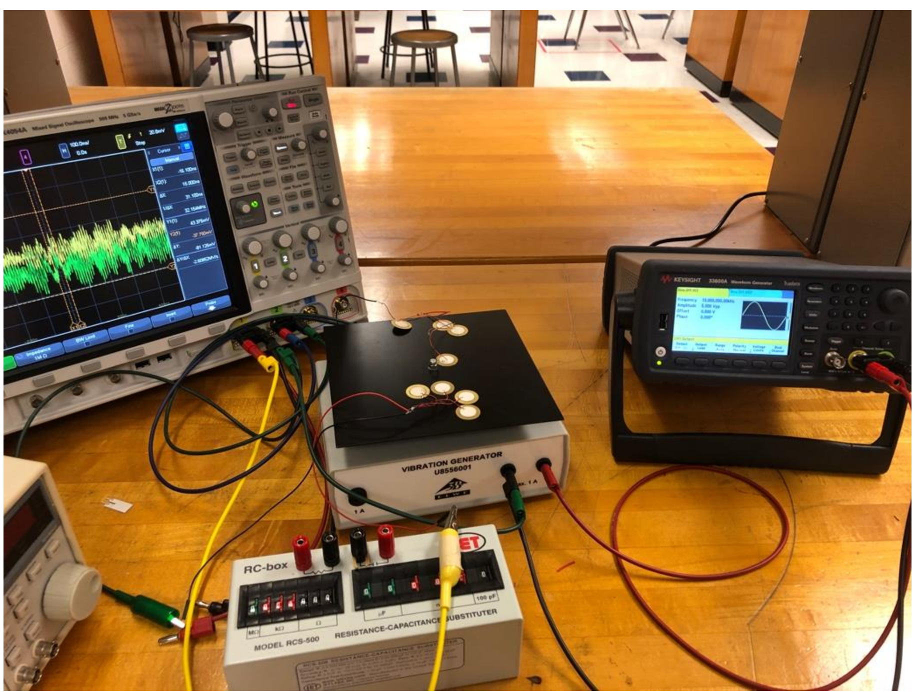

Figure 16: Illustration of experimental setup

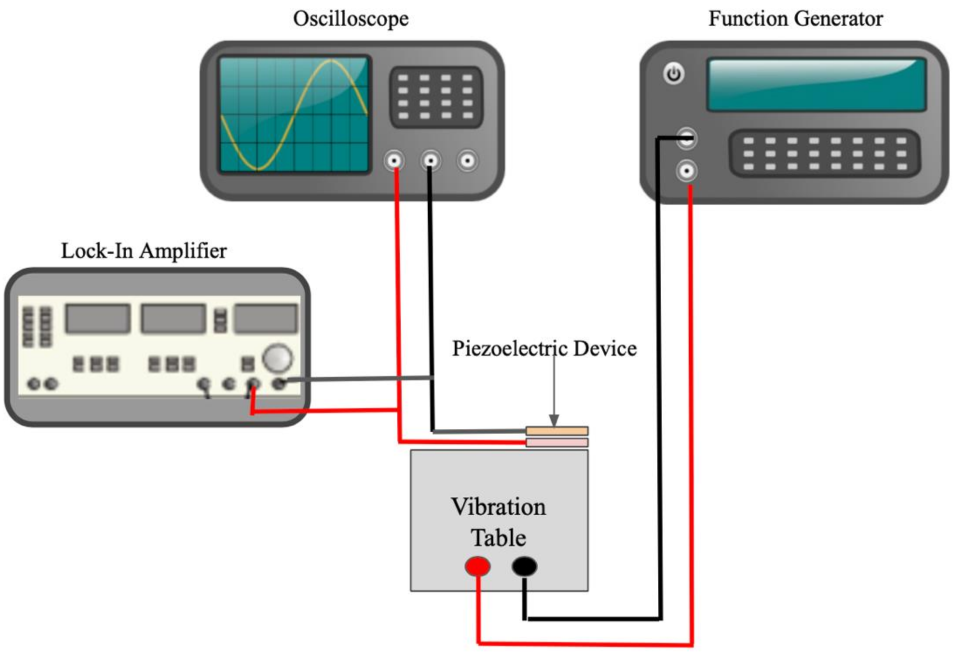

Figure 17: Block Diagram of setup

The sync function on the oscilloscope is connected to the reference bnc connector on the Locked-In amplifier. The amplifier Channel 1 is connected to the oscilloscope while the aux A/I is connected to the piezoelectric configurations.

In order to determine the maximum power of the piezoelectric arrays, the experiment replaces the single device with four of the same components connected in two different wiring configurations as shown in Figure x. The output responses of the device are recorded and investigated.

The intervals of the frequency ranged incrementally from 100 Hz to 100 kHz and the response of the output voltage was recorded.

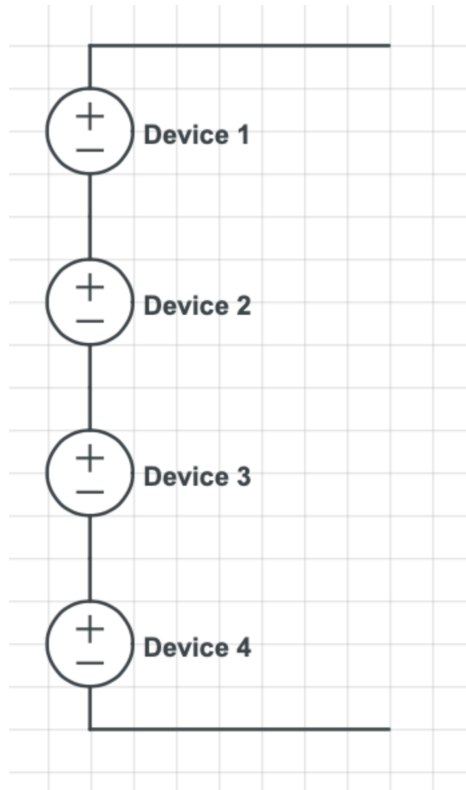

(a) Series

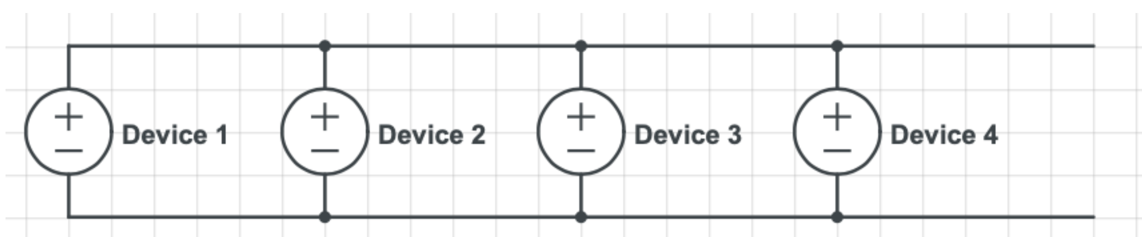

(b) Parallel

Figure 18: Piezoelectric configurations for (a) Series and (b) Parallel connections

Now using the same setup with a resistor decade box, the frequency is set to that of the resonant frequency of the device.

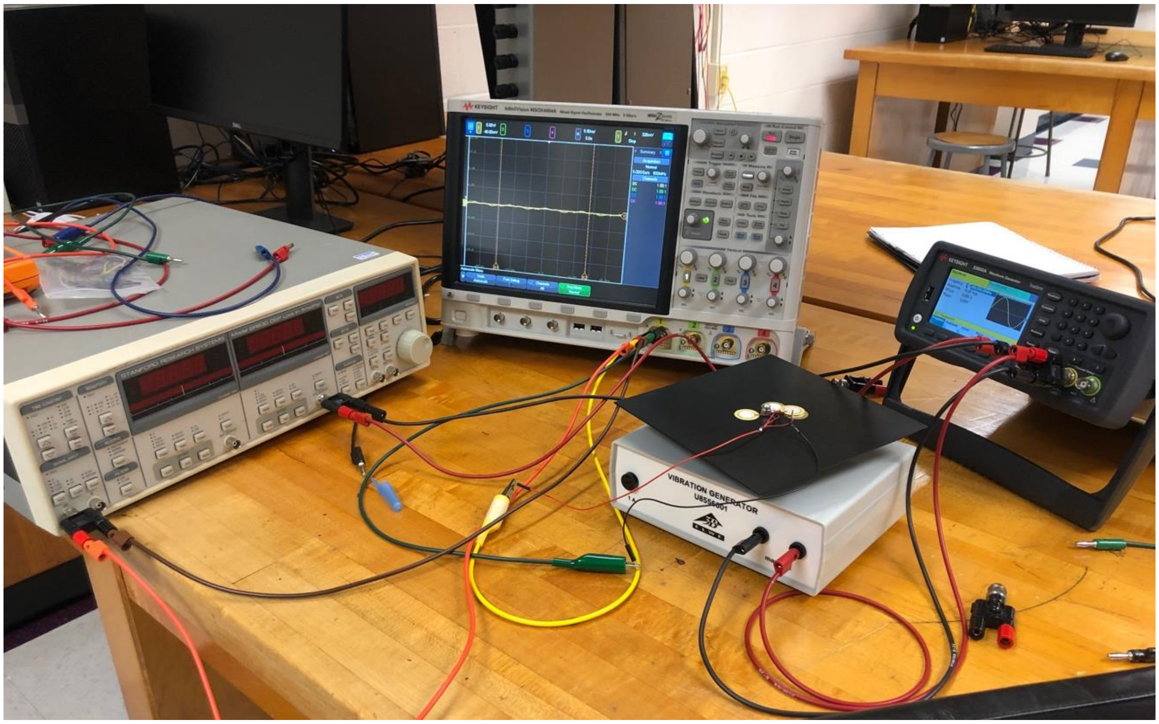

Figure 19: Illustration of the second experiment

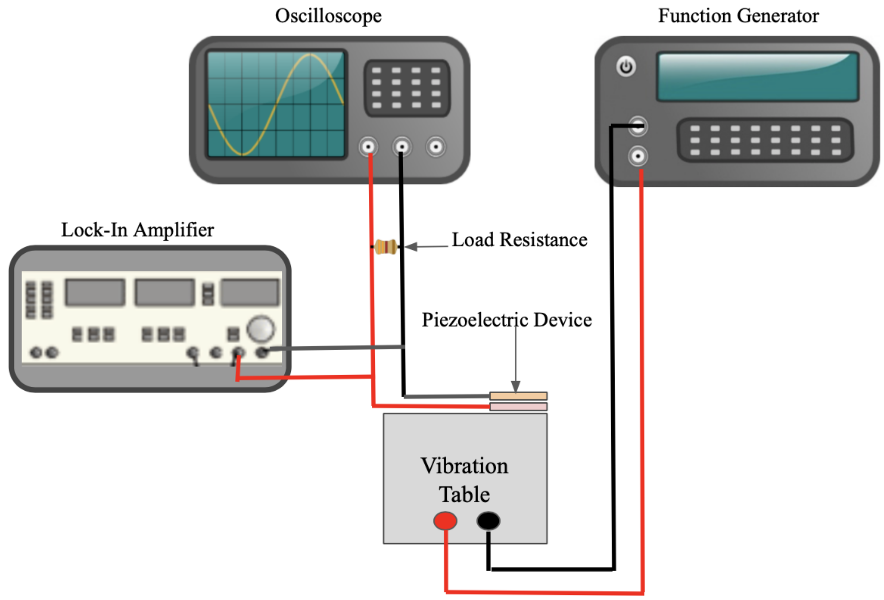

Figure 20: Block Diagram of experiment 2

Keeping the frequency consistent at the resonance of the individual piezoelectric device in the parallel configurations indicate an increasing sweep upwards. Once the load resistance is matched at 1200 kOhms the curve begins to saturate at a higher load resistance value. The small parallel piezo produced a maximum voltage of 9V peak to peak. While the larger piezoelectric connected in the same configuration produced a voltage of 6.13V peak to peak. The series connections produced a voltage peak for the smaller component at 10,.13 while the larger device reached a peak of roughly 8V as demonstrated in Figure 24 and Figure 25.

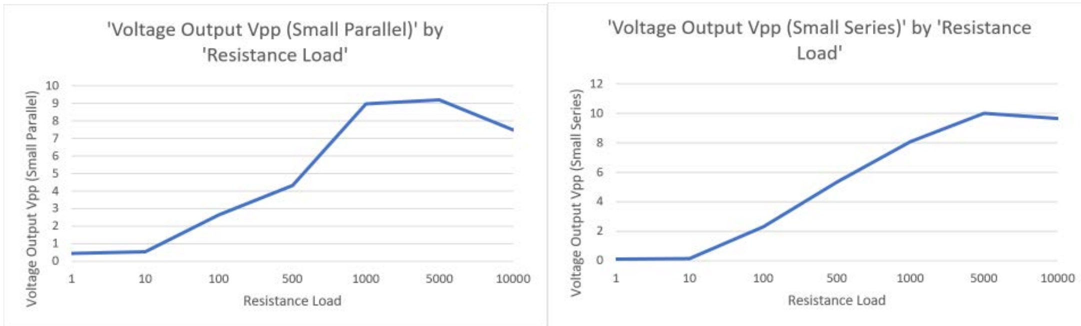

Figure 21: Output Voltage Response vs Load Resistance (Parallel Configuration)

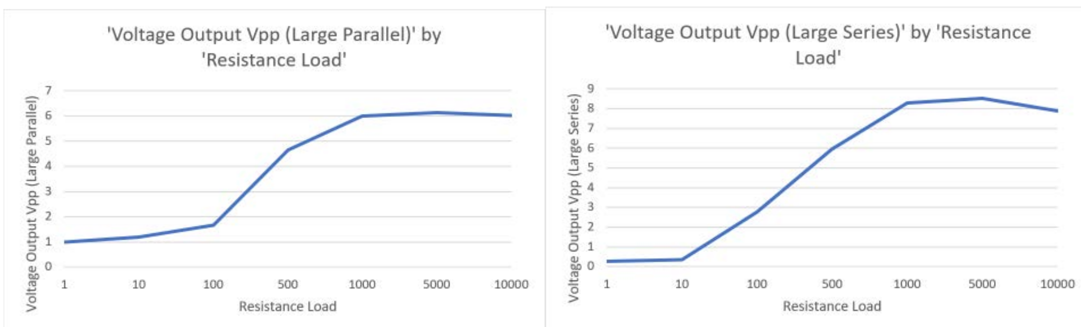

Figure 22: Output Voltage Response vs Load Resistance (Series Configuration)

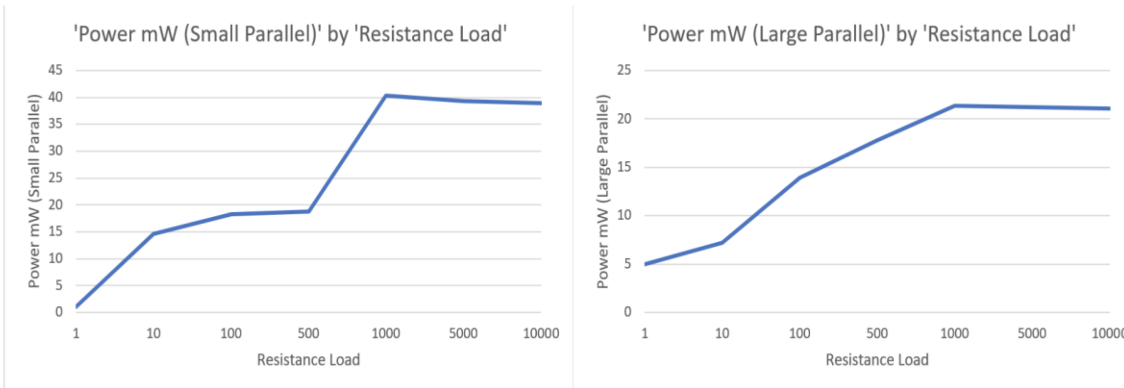

Figure 23: Output Power vs Resistance Load (Parallel Configuration)

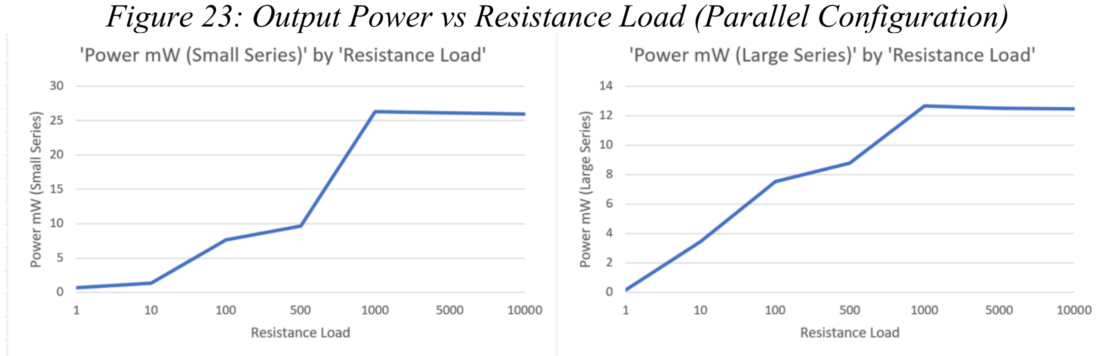

Figure 24: Output Power vs Resistance Load (Series Configuration)

For Figures 21-24, the frequency remained at 9kHz the resonance frequency of the piezoelectric components.

4.3 Results

The results obtained in the experiment were an attempt to investigate the voltage output change with respect to the configurations. Higher voltage levels are obtained from the piezoelectric components wired in series while a higher power output is generated from the parallel configuration. Based on the results outlined the max peak power is at the load resistance. For the parallel configurations the max output power was 21.34 mW (Large) and 40.31 mW (Small) respectively. While the series configurations were at 26.3 mW for small piezoelectric components and 12.67 mW. This is demonstrated in Figures 26 & 27. The max power will decrease as the current drops in the series connection. This is a result of the coupling factor from the piezoelectric device. To obtain a higher output power the piezoelectric constant and coupling factor needs to be improved. The charge accumulated from the direct piezoelectric effect will travel through another piezoelectric component as nothing is storing it when it is connected. Thus, one cannot assume the way to improve output power performance is from connecting more devices.

Chapter 5 Conclusion

5.1 Final Remarks

Piezoelectric components are a great selection as a power generator from both ambient and artificial sources that can be used for energy harvesting systems. Three methods of energy harvesting were analyzed and explored for energy harvesting. These methods consisted of piezoelectric, electrostatic, and electromagnetic applications. The scope of this researched is limited to piezoelectricity and vibration as the main source of excitation since it naturally exists in the environment. The excitation will generate power that can be used for small low power devices. In some applications, the power is harvested and stored into a capacitor until there is enough power to discharge for the application.

The connections of the piezoelectric device are extremely important to enhance the output power result. There are several factors to take into consideration in addition to the material type, geometry of the piezoelectric, and the amount of force applied. The direction of the applied force exists in multiple mode configurations that orient the dipoles in a particular direction. It was found the d33 mode configuration in previous research highlighted the increase in voltage performance. Additionally, the material layers of the bimorph indicated a higher voltage output compared to the unimorph counterpart.

It is difficult to classify and characterize some of the experimental data obtained from other studies in part because many are constructed in various shapes, size, materials, and the mode of operation that is applied. Therefore, with more variable parameters it is viable to see data in other literature reviews to vary. The company does not provide the exact material in the data sheets, thus making it harder to classify the piezoelectric performance. The power output shares no relationship with the volume size. In addition, energy harvester performance does not only rely on the conversion efficiency and power output. Analyzing results from similar geometrical but different material backgrounds indicate efficiency to be over 80% while other studies concluded that number to be less than 1%. Similarly, power output performance is not the only thing researchers want to pursue. If a universal standard was adopted, it would be considerably easier to classify these components.

This analysis is based on the consideration of the balance of charges, energy and electromechanical dynamics. In addition, the results are explained by the equivalent impedance approach. It shows a key difference in the analysis between series connection and parallel connection of multiple piezoelectric components. A unimorph device of two different size configurations were reviewed. The results discussed in Chapter 4 are similar to what was concluded in other forms of research. There are some discrepancies in the data and to improve the accuracy of the data, below are suggestions for further research.

These remarks to discuss the energy harvesting capabilities suggests others to review on the shelf piezoelectric devices instead of fabricating simulations. It may be easier to classify similar data if more experimentation was conducted on those particular pieces. Although this particular topic is extensively studied, there is still a considerable discrepancy between the expected performance and that of the achieved output.

Additionally, since this is an analysis of vibration, there are external vibration sources that contribute to the output on the oscilloscope. Vibrations naturally exist in the floor, wall, ceiling, and other room acoustics have a huge impact on the measurements. For future recommendation, it may be more efficient and accurate if data is obtained if the device under test is in an anechoic chamber.

In conclusion, the results expected were relatively close to what the theoretical results were to be from previous studies. However, discrepancies in data are a result from a non-uniform or universal standard. Overall, it is proven to have a substantial power performance difference with the parallel configuration compared to the series connection.

Bibliography

[1] Balpande, S.S. and Pande, R.S., 2015. Design and Simulation of MEMS Cantilever BasedEnergy Harvester-Power Source for Piping Health Monitoring System. 2015 National Conference on Recent Advances in Electronics & Computer Engineering (RAECE), Roorkee, pp.183–188.

[2] Bourgoine, N. (2011, April). Harvest Energy from a Single Photovoltaic Cell. Retrieved from https://www.analog.com/media/en/technical-documentation/tech-articles/lt-journal-article/LTJournal-V21N1-01-df-LTC3105-Nathan_Bourgoine.pdf

[3] BU-201: How does the Lead Acid Battery Work? (2011). Retrieved from https://batteryuniversity.com/learn/article/lead_based_batteries

[4] Covaci, C., & Gontean, A. (2020, June 21). Piezoelectric Energy Harvesting Solutions: A Review. Retrieved November 23, 2020, from https://www.mdpi.com/1424-8220/20/12/3512/htm

[5] Dakhole, A., & Boke, A. (2017, April). Electrical Energy Harvesting From Mechanical Pressure of Vehicles Using Piezoelectric Generators. Retrieved from https://pdfs.semanticscholar.org/6791/5dddd24288f35abb6f7a9b4edd52107cf083.pdf

[6] Edn. (2017, February 28). Introduction to lithium-ion rechargeable battery design. Retrieved September 9, 2020, from https://www.edn.com/introduction-to-lithium-ion-rechargeable-battery-design/

[7] Effects of battery manufacturing on electric vehicle life-cycle greenhouse gas emissions. (2018, February). Retrieved from https://theicct.org/sites/default/files/publications/EV-life-cycle-GHG_ICCT-Briefing_09022018_vF.pdf

[8] Electronic Components. (n.d.). Retrieved November 23, 2020, from https://www.mouser.com/ProductDetail/Mide/S118-J1SS-1808YB?qs=9r4v7xj2LnlK6yfRfh%2BLlA

[9] Enescu, D. (2019, January 21). Thermoelectric Energy Harvesting: Basic Principles and Applications. Retrieved November 23, 2020, from https://www.intechopen.com/books/green-energy-advances/thermoelectric-energy-harvesting-basic-principles-and-applications

[10] Hooker, M. (1998, September 1). NASA Technical Reports Server (NTRS). Retrieved November 13, 2020, from https://ntrs.nasa.gov/citations/19980236888

[11] German, J., Mock, P., Bandivadekar, A., Tietge, U., & Ligterink , N. (2017, November). FROM LABORATORY TO ROAD A 2017 UPDATE OF OFFICIAL AND "REAL-WORLD" FUEL CONSUMPTION AND CO2 VALUES FOR PASSENGER CARS IN EUROPE. Retrieved from https://theicct.org/sites/default/files/publications/Lab-to-road-2017_ICCT-white paper_06112017_vF.pdf

[12] J. Kymissis, C. Kendall, J. Paradiso, and N. Gershenfeld, "Parasitic power harvesting in shoes", Proc. 2nd IEEE ISWC, pp. 132-139, 1998

[13] Jia, Y., & Seshia, A. (2015, October 26). Ower Optimisation by Mass Tuning for MEMS Piezoelectric Cantilever Vibration Energy Harvesting. Retrieved from https://publications.aston.ac.uk/id/eprint/40391/1/4MC_JMEMS_pdf.pdf

[14] Jing, B. Y., & Leong, K. S. (2017). (PDF) Power Optimization Configuration for Piezoelectric ... Retrieved November 5, 2020, from https://www.researchgate.net/publication/317262241_Power_Optimization_Configuration_for_Piezoelectric_Cantilever_Arrays

[15] Liu, H., Zhong, J., & Lee, C. (n.d.). A comprehensive review on piezoelectric energy harvesting technology: Materials, mechanisms, and applications. Retrieved from https://www.ece.nus.edu.sg/stfpage/elelc/Publication/2018/APR_18V5_041306_ A comprehensive review on piezoelectric energy harvesting technology Materials, mechanisms, and applications.pdf

[16] Lefeuvre, A. Badel, C. Richard, and D. Guyomar, "Piezoelectric Energy Harvesting Device Optimization by Synchronous Electric Charge Extraction", J. of Int. Material Systems & Structures, vol. 16, pp. 865 – 876, 2005.

[17] Ottman, G. K.; Hofmann, H. F.; Bhatt, A. C. and Lesieutre, G. A. Adaptive piezoelectric energy harvesting circuit for wireless remote power supply. IEEE Trans. Power Electron., 17(5), 2002, pp.669-676.

[18] Piezoelectricity. (n.d.). Retrieved November 13, 2020, from https://www.americanpiezo.com/knowledge-center/piezo-theory/piezoelectricity.html

[19] Rahim, R. (2013, December). Acoustic Energy Harvesting Using Piezoelectric Generator ... Retrieved November, 2020, from http://www.enggjournals.com/ijet/docs/IJET13-05-06-118.pdf

[20] Roundy, S., Wright, P.K and Rabaey, J., "A study of low level vibrations as a power source for wireless nodes," Computer Communications, Vol.26, pp.1131-1144,2003

[21] Rusu, C. (2019, December 31). Theory: How to Calculate Piezoelectric Material Properties from a Material Datasheet. Retrieved November 13, 2020, from https://onscale.com/blog/theory-how-to-calculate-piezoelectric-material-properties-from-a-material-datasheet/

[22] S. P. Mohanty, Nanoelectronic Mixed-Signal System Design, no. 9780071825719, McGraw-Hill Education, 2015.

[23] SparkFun Electronics: Optoelectronics: DigiKey. (n.d.). Retrieved November 2, 2020, from https://www.digikey.com/en/products/detail/sparkfun-electronics/COM-11120/5673801

[24] T.H. Ng, and W.H. Liao, "Sensitivity Analysis and Energy Harvesting for a Self-Powered Piezoelectric Sensor", J. of Int. Material Systems & Structures, vol. 16, pp. 785-797, 2005

[25] Thiruvelselvam, Senthil, K. (2018, April). Energy Harvesting From A Piezoelectric Source To Power A Wireless System. Delft University of Technology, Netherlands.

[26] TECHNICAL NOTE 32 - Statek Corporation. (n.d.). Retrieved November 23, 2020, from http://statek.com/wp-content/uploads/2018/03/tn32.pdf

[27] Tsukamoto, T., Umino, Y., Shiomi, S., Yamada, K., & Suzuki, T. (2018). Bimorph piezoelectric vibration energy harvester with flexible 3D meshed-core structure for low frequency vibration. Science and technology of advanced materials, 19(1), 660–668. https://doi.org/10.1080/14686996.2018.1508985

[28] Wang, Z., Pan, X., He, Y., Hu, Y., Gu, H., & Wang, Y. (2015, June 25). Piezoelectric Nanowires in Energy Harvesting Applications. Retrieved November 23, 2020, from https://www.hindawi.com/journals/amse/2015/165631/

[29] Worthington, E. (2010, March 10). Piezoelectric energy harvesting : Enhancing power output by device optimisation and circuit techniques. Retrieved September 22, 2020, from https://core.ac.uk/display/40033699

[30] Yang, Zhengbao, et al. "High-Performance Piezoelectric Energy Harvesters and Their Applications." Joule, vol. 2, no. 4, Apr. 2018, pp. 642–97, doi:10.1016/j.joule.2018.03.011.

[31] Zheng, Qinglong, et al. "Vibration Energy Harvesting Device Based on Asymmetric Air-Spaced Cantilevers for Tire Pressure Monitoring System." Proceedings of Power MEMS, 2009, pp. 403–406.